ISBN: 978-3-95450-241-7 ISSN: 2673-5350 doi:10.18429/JACoW-IBIC2022-TUP25

SIMULATION AND MEASUREMENTS OF THE FAST FARADAY CUPS AT GSI UNILAC

R. Singh*[1], S. Klaproth[2], P. Forck[1], T. Reichert[1], A. Reiter [1], G. Rodrigues[3]
[1]GSI Helmholtz Center for Heavy Ion Research, Darmstadt, Germany
[2]Technische Hochschule Mittelhessen, Friedberg, Germany
[3]Inter University Accelerator Center, New Delhi, India

Abstract

The longitudinal charge profiles of the high intensity heavy ion beam accelerated at the GSI UNILAC up to 11.4 MeV/u can differ significantly in consecutive macro-pulses. Variations in bunch shape and mean energy were also observed within a single macro-pulse. In order to have an accurate and fast determination of bunch shape and its evolution within a macro-pulse, a study of fast Faraday Cup designs is underway at GSI. In this contribution, we present CST particle in cell (PIC) simulations of radially coupled co-axial Fast Faraday Cup (RCFFC) and conventional axially coupled FFC (ACFFC) design. The simulation results are compared to the measurements performed under comparable beam conditions primarily with RCFFCs. A rather large impact of secondary electron emission is observed in simulations and experiments. The biasing of the FFC central electrode as a mitigation mechanism on the measured profiles is discussed.

INTRODUCTION

Measurement of longitudinal beam parameters such as kinetic energy, the energy spread, and spread in particle time of arrival with respect to the RF is essential in linear accelerators (LINACs). Kinetic energy measurements are performed using the Time of Flight (ToF) between two or more phase probes (also referred as pick-ups/BPMs) and are routinely done at several locations along the UNILAC. The correlated distributions of beam energy spread and time of arrival with respect to RF phase or "phase spread" with respect to synchronous particle form an ellipse in longitudinal phase space. Typical strategy of determining full longitudinal phase space ellipse is by measuring one of the projection of longitudinal phase space under controlled longitudinal optics settings [1]. The problem of longitudinal emittance determination is thus reduced to precise measurement of the longitudinal charge distribution. The measurement of phase/time of arrival spread also referred to as "longitudinal charge distribution" or often just "bunch length" or "bunch shape" and is typically more accessible for direct measurements. Fast Faraday cups (FFCs) are variants of the regular Faraday cups optimized for measuring fast time varying charge distributions. In order to measure short bunch signals in ns regime, the FFC structures are carefully designed to match the signal termination impedance along with measures for suppression of field dilution and secondary electrons.

In this upcoming section, we will show the simulations of two FFC designs, a) in the first design, the beam is radially coupled into a coaxial cable via a blind hole [2] which is compared with a second design b) the traditional and commercially available axially coupled tapered co-axial cable design [3]. The simulation details and signals induced by beam in the FFC structure in presence of secondary electron emission are discussed. In the following section, measurements with ion beam performed with these FFCs are discussed.

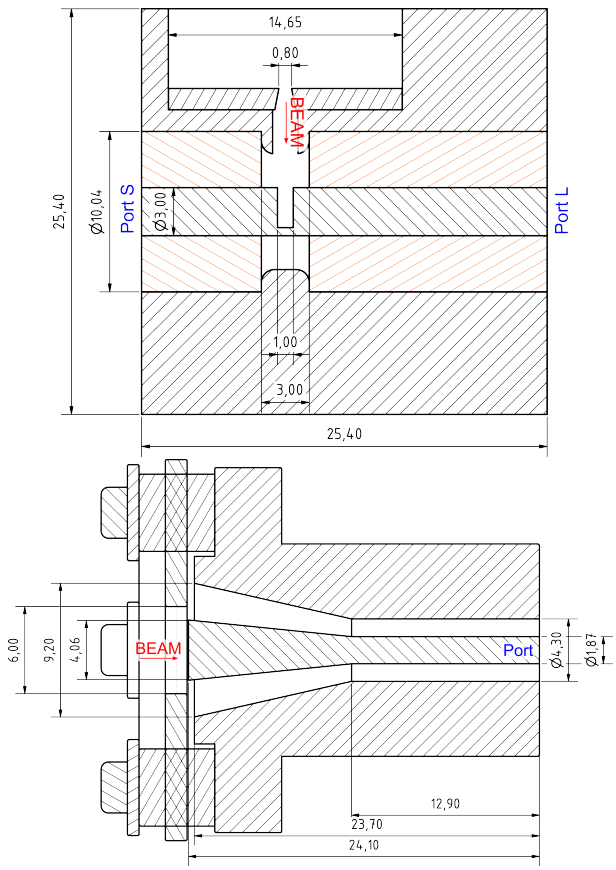

Figure 1: Schematic of the two co-axial FFCs investigated in this manuscript. (Top) Radially coupled FFC and (bottom) Axially coupled FFC. The beam incidence and port for signal coupling are indicated.

SIMULATIONS

Both FFC designs are shown in Fig. 1 which are simulated with the PIC solver of CST EM Studio and ion beam as input.

* r.singh@gsi.de

ISBN: 978-3-95450-241-7 ISSN: 2673-5350 doi:10.18429/JACoW-IBIC2022-TUP25

In addition to ensuring matched signal transmission, these simulations study the deformations in the measured time structure of the beam due to secondary electron yield and field elongation for non-relativistic ion beams.

The first design (RCFFC) where beam enters radially into the co-axial structure is shown in Fig. 1 (top). The basic idea behind the design is coupling of beam through a blind hole from the side of a co-axial through the dielectric medium into the central conductor. The choice of hole width (1 mm) and depth (2.8 mm) is to minimize the escape of emitted secondary electrons. The blind hole in the central conductor of the co-axial is covered with a Titanium Zirconium Molybdenum Alloy (TZM) disk with a small 0.8 mm hole with the dual purpose of reducing field dilution effects [4] and tolerating the heat deposited by the beam. A detailed discussion of the design can be found here [2]. A modification of this design geared towards lower intensity beams is discussed in another contribution of this conference [5]. The second

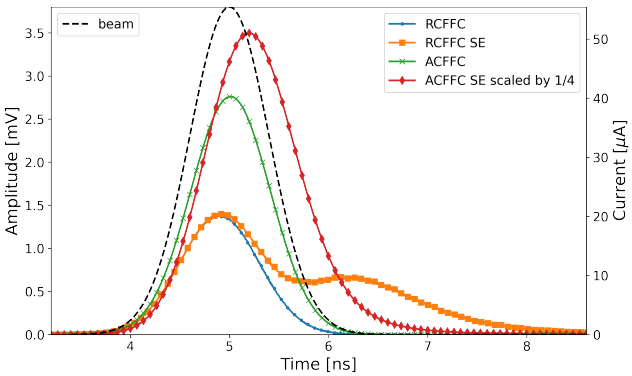

Figure 2: Induced signal with and without secondaries for both FFC designs ($\beta = 0.15$, $\sigma = 400$ ps).

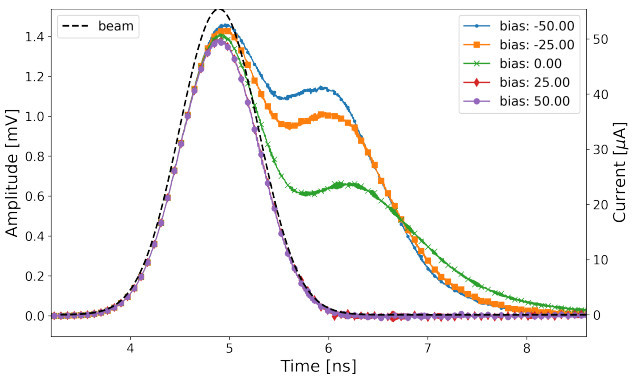

Figure 3: The effect of biasing on the induced signal for radially coupled FFC ($\beta = 0.15$, $\sigma = 400$ ps).

FFC design is the traditional open ended tapered axially coupled co-axial structure [3] shown in Fig. 1 (bottom). The core idea is to enlarge the co-axial cable via a taper while maintaining 50 Ω impedance. There is a grid in front to avoid passage of the beam pre-field which leads to dilution of the measured profile. A comparable design is available on loan from Bhabha atomic research center (BARC) and was used for some of the verification measurements.

The ion induced secondary electron yield and energy spectra have been widely studied in literature [6–9] and some recent studies in context of secondary electron grids for transverse profile measurement of ion beams are discussed here [10]. The backward secondary electron yield per incident ion can be estimated using the Bethe-Bloch formula for the stopping power of charged particle beam on a target. The number of secondary electrons N_e is thus proportional to the square of charge state Z of the incident ion and target electron density n of the FFC material.

$$N_e \propto nZ^2 \cdot N_{ion} \quad (1)$$

Empirical estimates from literature suggest emission of about 10-15 e^- for 8.0 MeV/u O^{5+} ion normally incident with energy of on a copper target [8, 11, 12]. For 8.6 MeV/u Ar^{10+}, this gives about 50 e^- per incident ion and this estimate has been used in our simulations. The secondary electron yield also has a strong dependence on the angle of incidence with respect to surface normal θ. For smooth surfaces the yield is proportional to sec θ [13]. Even for normally incident beam $\theta = 0$, the roughness of the surface could lead to an increased secondary yield due to random distribution of incidence angles, however this effect is not considered in this paper. The secondary electron emission from the surface follows a cosine distribution with respect to target normal [14]. For the radially coupled FFC discussed above with 1 mm diameter and 2.5 mm depth, about 15 % of electrons should exit the blind hole potentially causing the deformation in the induced signal. The energy spectra of the majority of secondary electrons is known to below 50 eV [15, 16]. The secondary electron energy spectra simulated in CST uses the Vaughan model parameterisation [17]. The simulation results showing the induced signal for a longitudinal charge distribution with $\sigma = 400$ ps for $\beta = 0.15$ with and without secondaries for both FFC designs are shown in Fig. 2. There is a clear deformation of induced signal on the FFC for both designs with the secondaries. That is related to the secondary electron emission and the time these low energy electrons require to leave the area near the central conductor of the FFC. Figure 3 shows the effect of biasing the central conductor for radially coupled FFC under different bias voltages. It is clear that +ve bias on the central conductor suppresses the electrons leaving the blind hole and deformation of the induced signal. The field dilution effect is not visible for 400 ps bunches, and becomes more relevant for shorter bunches, e.g. < 100 ps especially for ACFFC.

EXPERIMENTS

Most of the measurements were performed with the radially coupled FFC at the exit of the X2 beam line with ion beam energy of 8.6 MeV/u. Previous measurements with a beam of lower energy and charge state and a comparison of the FFC with a Feschenko monitor are reported here [18]. These measurements were performed with a DC biasing scheme of the FFC central conductor as shown in Fig. 4. Biasing is performed to influence the motion of secondary

ISBN: 978-3-95450-241-7 ISSN: 2673-5350 doi:10.18429/JACoW-IBIC2022-TUP25

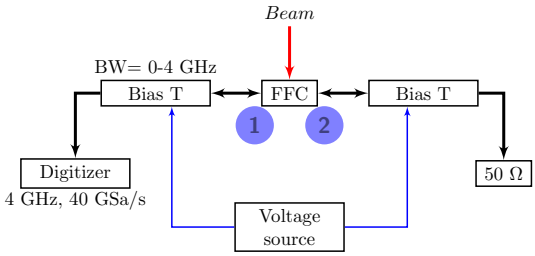

Figure 4: The symmetric biasing scheme ensures that there is no current flow through the FFC due to the biasing.

electrons emitted due to the beam irradiation. The biasing scheme ensures that no DC current flows through the FFC due to the bias voltage. This first measurement was performed with a 0.4 mA O^{6+} beam in 2021 campaign and the bunch length evolution along the full macro-pulse is shown in Fig. 5 for three bias settings. For case with zero biasing voltage, we observe a significant bunch "tail" of around 3 ns in the measured profile. The tail was suppressed on application of +ve bias and is further increased on application of −ve bias inline with the simulations. Although the electrons are created almost instantaneously after the beam hits the central conductor, the additional signal due to electron emission is only induced after electrons leave the blind hole as discussed earlier. 1 - 10 eV electrons possess a velocity of 0.6 to 2 mm/ns and need between 1 - 3 ns to exit the blind hole in the central conductor forming the long tail. There is a reflection at around 40 degrees which vanishes when the biasing scheme was removed. Fig. 6 shows the averaged bunch calculated for the whole macro-pulse. The second smaller peak is clearly visible along with the reflection as annotated in the plot.

Similar measurement was performed with Ar^{10+} beam also at 8.6 MeV/u in the 2022 campaign where the machine settings were different. The averaged bunch shape measurement in a 50 µs pulse as a function of DC bias applied on FFC central conductor is shown in Fig. 7 (top). The Phase Probe (PP) signal installed 0.5 m upstream of the FFC is shown in Fig. 7 (bottom) and shows that the beam conditions were stable during the measurement. Typically convolution of FFC signal with the field elongation expression can be used to estimate the true charge state distribution [4].

The charge profile measured by FFC were compared with the phase probe signal. Figure 8 shows the estimated bunch width (4σ) as a function of bias voltage after erasing the signal below 10 % of maximum amplitude. The bunch width seems to saturate around 30 V. Other measurements reported in literature [3, 10] suggest that more than 90 % electrons have energies below 30 eV and 30 - 50 V DC bias should be sufficient to suppress the signal distortion due to secondary emission. Figure 9 shows the comparison of ACFFC and RCFCC under comparable machine settings. We should however note that due to unavailability of sufficient feedthroughs, the measurements with the two FFCs were done on different days. The ACFFC consistently shows

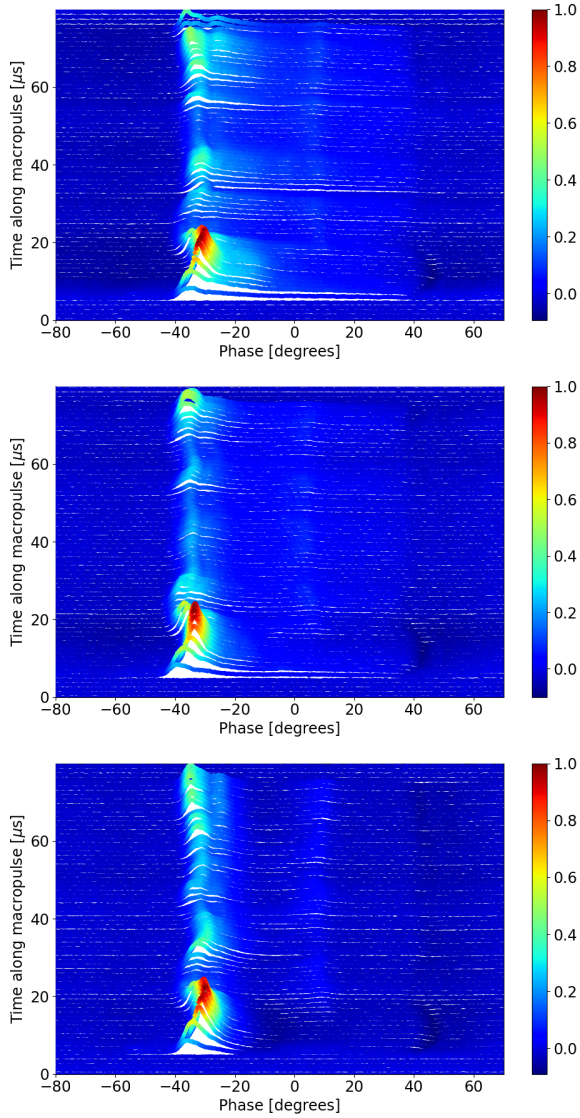

Figure 5: The waterfall plot showing the full macro-pulse for various DC bias voltages applied on central conductor of the radially coupled FFC −25 V (top) 0 V (middle) and 25 V (bottom).

a dip at the tail of bunch and seems to be less affected by secondary emission. Currently, it is speculated that the dip at the end is caused by particles which interact with central conductor of ACFFC due to its pre-field but are not deposited on it causing a phase probe like behavior.

CONCLUSION

We have studied two FFC designs by means of CST simulations taking the secondary emission and external biasing voltage into account. Measurements under similar beam conditions are reported where a strong distortion in the longitudinal charge profile measurement due to secondary electrons is observed. External DC biasing of central conductors is shown to mitigate the distortion to a large extent.

ISBN: 978-3-95450-241-7 ISSN: 2673-5350 doi:10.18429/JACoW-IBIC2022-TUP25

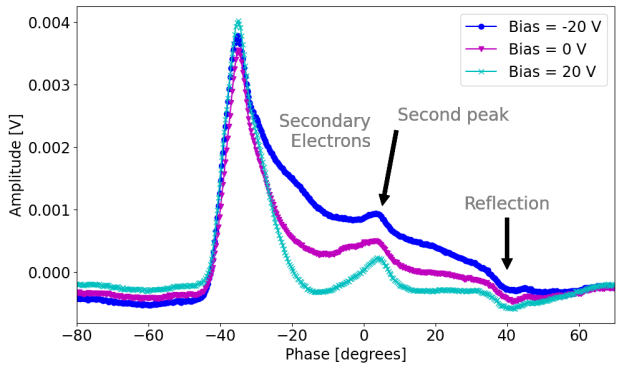

Figure 6: The longitudinal charge profile measurement averaged for a macro-pulse with application of various DC bias voltages on the radially coupled FFC central conductor.

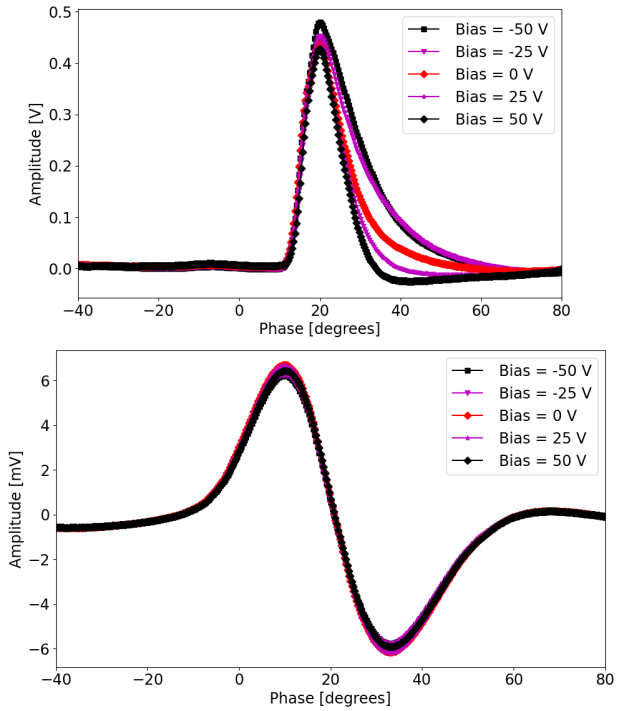

Figure 7: The FFC and preceding phase probe signal for various bias voltages.

ACKNOWLEDGEMENTS

This work is supported by the German Federal Ministry of Education and Research (BMBF) under contract no. 05P21RORB2. Joint Project 05P2021 - R&D Accelerator (DIAGNOSE). R. Singh and G. Rodrigues acknowledge the support received under VAJRA project (VJR/2018/000115) from Department of Science and Technology, India. D. Sun, A. Shemyakin and V. Scarpine are gratefully acknowledged for providing the RCFFC on loan. We thank J. Matthew for providing the ACFFC on loan.

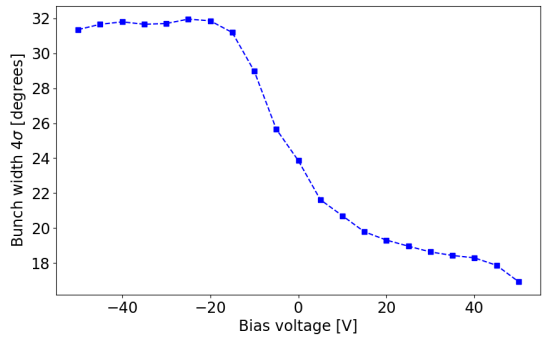

Figure 8: The longitudinal charge profile measurement averaged for a macro-pulse with application of various DC bias voltages on the FFC central conductor.

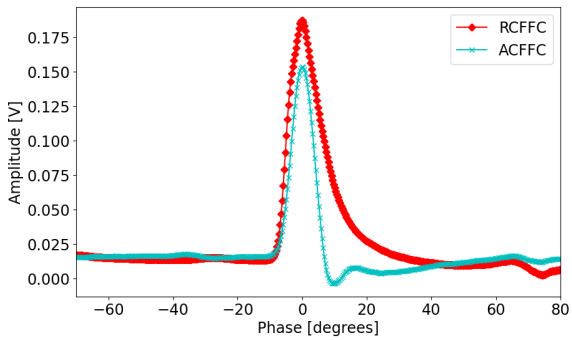

Figure 9: Bunch shape measurements comparison between the axially coupled coaxial structure and the radially coupled coax FFC under comparable machine settings without any biasing.

REFERENCES

[1] S. Lauber *et al.*, "Longitudinal phase space reconstruction for a heavy ion accelerator", *Phys. Rev. Accel. Beams*, vol. 23, p. 114201. doi:10.1103/PhysRevAccelBeams.23.114201

[2] J.-P. Carniero *et al.*, "Longitudinal beam dynamics studies at the PIP-II injector test facility", *Int. J. Mod. Phys. A*, vol. 34, no. 36, 2019. doi:10.1142/S0217751X19420132

[3] W. R. Rawnsley *et al.*, "Bunch shape measurements using fast Faraday cups and an oscilloscope operated by LabVIEW over Ethernet", *AIP Conf. Proc.*, vol. 546, p. 547, 2000. doi:10.1063/1.1342629

[4] R. Singh, "Longitudinal diagnostics R&D at GSI UNILAC", in *Proc. HIAT'22*, Darmstadt, 2022, to be published.

[5] G. Rodrigues *et al.*,"Studies on Radially Coupled Fast Faraday Cups to Minimize Field Dilution and Secondary Electron Emission at Low Intensities of Heavy Ions", presented at the IBIC'22, Kraków, Poland, Sep. 2022, paper WEP28, this conference.

[6] E. J. Sternglass, "Theory of Secondary Electron Emission by High-Speed Ions", *Phys. Rev.*, vol. 108, no. 1, 1957. doi:10.1103/PhysRev.108.1

[7] H. Rothard *et al.*, "Secondary-electron yields from thin foils: A possible probe for the electronic stopping power of heavy

ISBN: 978-3-95450-241-7 ISSN: 2673-5350 doi:10.18429/JACoW-IBIC2022-TUP25

ions", *Phys. Rev. A*, vol. 41, no. 5, p. 2521, 1990. doi:10.1103/PhysRevA.41.2521

[8] A. Koyama, T. Shikata and H. Sakairi, "Secondary electron emission from Al, Cu, Ag and Au metal targets under proton bombardment", *Jpn. J. Appl. Phys.*, vol. 20, no. 1, pp. 65-70, 1981. doi:10.1143/JJAP.20.65

[9] D. Hasselkamp, K. G. Lang, A. Scharmann and N. Stiller, "Ion induced electron emission from metal surfaces", *Nucl. Instrum. Methods*, vol. 180, no. 2–3, pp. 349-356, 1981. doi:10.1016/0029-554X(81)90076-8

[10] A. Reiter *et al.*, "Investigation of Cross Talk in Secondary Electron Emission Grids", Technical Note LOBI-TN-SEM-2012-001, GSI, Darmstadt, 2012.

[11] O. Benka, A. Schinner, T. Fink and M. Pfaffenlehner, "Electron-emission yield of Al, Cu, and Au for the impact of swift bare light ions", *Phys. Rev. A*, vol. 52, no. 5, pp. 3959-3965, 1995. doi:10.1103/PhysRevA.52.3959

[12] A. F. Haque *et al.*, "Proton-induced secondary electron emission from elemental solids over the energy domain 1 keV–1000 MeV", *Results Phys.*, vol. 15, p. 102519, 2019. doi:10.1016/j.rinp.2019.102519

[13] D. Hasselkamp, H. Rothard, K. O. Groeneveld, J. Kemmler, P. Varga and H. Winter, "Particle Induced Electron Emission 2", vol. 4, p. 25, Springer-Verlag, Berlin/Heidelberg, 1992.

[14] H. Rothard *et al.*, "Differential multi-electron emission induced by swift highly charged gold ions penetrating carbon foils", *Nucl. Instrum. Methods Phys. Res., Sect. B*, vol. 258, pp. 91–95, 2007. doi:10.1016/j.nimb.2006.12.132

[15] D. Hasselkamp, S. Hippler and A. Scharmann, "Ion induced secondary electron spectra from clean metal surfaces", *Nucl. Instrum. Methods Phys. Res., Sect. B*, vol. 18, pp. 561-565, 1987. doi:10.1016/S0168-583X(86)80088-X

[16] N. V. Sydorenko, S. I. Kononenko and V. P. Zhurenko, "Mean energy of electrons emitted from solid unders swift light ion bombardment", *Journal of Kharkiv University*, no. 657, pp. 81-84, 2005.

[17] J. R. Vaughan, "Secondary Emission Formulas", *IEEE Trans. Electron Devices*, vol. 40, no. 4, 1993. doi:10.1109/16.202798

[18] R. Singh *et al.*, "Comparison of Feschenko BSM and Fast Faraday Cup with Low Energy Ion Beams", in *Proc. IBIC'21*, Pohang, Korea, Sep. 2021, pp. 407–411. doi:10.18429/JACoW-IBIC2021-WEPP16